



# Open-pore morphology of *i*-PP copolymer crystallized from a gel state in supercritical propane

Souvik Nandi<sup>a</sup>, H. Henning Winter<sup>a,\*</sup>, H.G. Fritz<sup>b</sup>

<sup>a</sup>Department of Chemical Engineering, University of Massachusetts, Amherst, MA 01003, USA

<sup>b</sup>Institut für Kunststofftechnologie, University of Stuttgart, Stuttgart, Germany

Received 12 November 2003; received in revised form 27 April 2004; accepted 27 April 2004

## Abstract

Open-pore morphology was produced in low-density polypropylene (*i*-PP) by first crosslinking the *i*-PP and then crystallizing it from a highly swollen state in supercritical propane. The extent of crosslinking, expressed by an increasing gel fraction and an increasing compression modulus, was found to have a strong effect on pore size but less so on crystal structure. The resulting pore structure, studied using scanning electron microscopy, showed a decrease in pore size with an increase in gel fraction. Typical pore sizes are between 1 and 10  $\mu\text{m}$ . The polymer morphology in the wall, analyzed using wide-angle X-ray diffraction, indicated the presence of  $\alpha$ -PP crystals. The experimental results showed that mostly loose chains (sol fraction) contribute to the crystallinity of the polymer. For our specific *i*-PP, the crosslinked network devoid of sol fraction (after extraction) collapses during cooling and does not produce any open pore structure.

© 2004 Published by Elsevier Ltd.

**Keywords:** Open pores; Pore size; Supercritical propane

## 1. Introduction

There is need for a zero emission process that is able to generate open-pore polymers with large internal surface area. Average pore size and shape should be controllable. The process should avoid hazardous solvents and the resulting pore structure should be free of residues. Crystallization of polyolefins from a swollen crosslinked network (CSX) is such a process of making open-pore materials. The steps involved in the CSX process are explained in detail by Winter et al. [1]. The first figure in this publication [1] shows the sequence of processing steps in the pressure–temperature domain.

We do not have a clear understanding of the mechanism of pore formation during CSX. As a working hypothesis, we assume that the pore structure forms in the following way. Preshaped and crosslinked polymers are swollen in a supercritical fluid above the crystal melting temperature of the polymer. Supercritical propane (SCP) serves as a good swelling fluid for polypropylene (and polyethylene). The polymer in the swollen gel state is amorphous. Upon cooling below the crystallization temperature while maintaining

pressure, fractions of the polymer crystallize in a nucleation and growth process and phase-separate from the fluid. Large composition fluctuations develop by the crystallization action. As an alternative pore-formation mechanism, it is also conceivable that some of the polymer first separates from the fluid and then crystallizes. In either case, the result is a bicontinuous morphology in which one phase is polymer rich (crystalline polymer and polymer rich amorphous phase) and the other is mostly fluid. The swelling fluid creates a continuous fluid phase, which after its release leaves behind an open pore structure. SCP can be easily removed from the open pores by lowering the pressure. Such venting occurs preferably above the critical temperature of the fluid but below the melting temperature of the polymer. The propane can be cleaned and recycled into the CSX process. Crystallization introduces the rigidity transition that stabilizes the porous structure. For achieving a large void fraction in the final specimen, the major component of this 2-phase structure is the fluid. The crosslinking is assumed to play an important role in the phase separation process since it suppresses large-scale polymer diffusion during crystallization (which is known for polymer solutions to result in large-scale composition fluctuations and low mechanical strength).

An important intermediate state is the swollen polymer

\* Corresponding author.

E-mail address: [winter@ecs.umass.edu](mailto:winter@ecs.umass.edu) (H. Henning Winter).

(gel) that is needed for generating the rigid pore structure. The gel consists of a three-dimensionally crosslinked network polymer that has absorbed a large quantity of a solvent (swelling fluid). Flory [2] modeled the amount of swelling of a polymer network using the total free energy change involved in the mixing of pure swelling fluid with the initially unrestrained polymeric network. The total free energy is considered to consist of two parts: the ordinary free energy of mixing and the elastic free energy of the expanded network structure. The system we are working with is slightly more complicated. The polymer is only partially crosslinked and contains a polymer sol fraction that acts as an athermal solvent. Hence, the network interacts with both the athermal solvent and the swelling fluid, which contributes towards the total free energy of mixing. The elastic free energy is dictated by the expanding polymer network fraction only and not by the loose molecules. An increase in the crosslink density results in an increase in the number of effective network chains per unit volume in the polymer  $v_e$  and, hence, reduces the swelling. Swelling reaches its equilibrium when the chemical potential of the swelling fluid within the polymer network equals the chemical potential of the bulk solvent outside the polymer sample. A detailed study of this phenomenon is in progress.

In the CSX process, the rate and the total degree of swelling are controlled by the diffusivity of the fluid in the polymer, by sample size, and by the exposure time at elevated  $P$ – $T$  conditions. This exposure time (also called the ‘soak time’) is one of the dominating parameters for the CSX process. During soaking, while the small fluid molecules diffuse into the polymer, unattached polymer molecules (sol fraction) are able to diffuse out of the sample into the surrounding fluid. Here, the diffusivity of the swelling fluid is much higher than that of the loose polymer molecules. Thus although a real equilibrium cannot be reached in the short cycle time of the CSX process, the system can be considered to be in a quasi-steady-state at every instant in time.

Crystallization from the gel state is similar, in many aspects, to crystallization from solution. Porous structure can be obtained by crystallizing polyolefins from supercritical solutions [3–5]. Whaley et al. [3,4] studied the crystallization of *i*-PP from supercritical solution at different crystallization temperatures. The most common morphology observed is that of porous microspheres having a spherulitic habit whose sizes range from 50 to 150  $\mu\text{m}$  but can be significantly larger. Han et al. [5] also studied the morphology obtained from the rapid expansion of supercritical solution and isobaric crystallization from supercritical solution (ICSS) of *i*-PP and ethylene–butene (EB) copolymer. They observed that the ICSS process produced microcellular polymeric foamlike materials by thermally induced crystallization below the solid–liquid transition temperature. In case of crosslinked network polymers, spherulitic growth is also expected. The loose chains and the network might co-crystallize to form the porous structure.

It is also possible that the polymer network consists of a high density of defects, which hinder it from forming an ordered structure and crystallize. In such a situation, the sol molecules crystallize in the presence of the amorphous matrix of the network.

This study on the pore formation by the CSX process focuses on the effect of crosslink density on the final structure, the pore size, and the void fraction. Measurements will show the extent to which the network polymer crystallizes and participates in the pore formation process. Also the role of the sol fraction in this process is studied. Experiments have the purpose of identifying the competing phenomena, their dynamics, and their limiting conditions.

## 2. Experimental

### 2.1. Materials

The base polymer is the commercially available Hifax CA10 (Basell Polyolefins), a random block copolymer of *i*-PP and PE in which *i*-PP is the dominant component. The specific *i*-PP/PE ratio is unknown to us. The polymer chains also contain an unknown rubber phase ( $X_0$ ) (segments in the backbone or at the chain ends). Copolymer (PE segments) reduces the regularity of the molecular chains. The small amounts of polyethylene in its backbone, along with the synthetic rubber phase, reduce the size of the crystallizable blocks in *i*-PP molecules. This expresses itself in a low value of the differential scanning calorimetry (DSC) crystal melting point of 142  $^{\circ}\text{C}$  and low crystallinity of about 12%.

The polymer was prepared in a twin-screw extruder (ZSK30-Werner and Pfleiderer). Silane groups in the form of vinyl trimethoxy silane (VTMOS) were grafted to the backbone chain using dicumyl peroxide (DiCUP) as initiators at compositions according to Table 1. Radicals generated by the thermal decomposition of DiCUP initiate a removal of hydrogen atoms from the tertiary or secondary C-atom from the backbone producing main chain radicals. Bifunctional VTMOS groups graft onto these chain radicals by a break-up of the vinyl double bond. The extent of crosslinking in each sample depends not only on the fraction of organosilane, VTMOS, but also on the amount of peroxide DiCUP. DiCUP plays an important role in the grafting process. A small amount of DiCUP produces too few grafts while a large amount of DiCUP creates chain scission in the *i*-PP backbone. An optimum amount of DiCUP is required for a successful grafting reaction. Added styrene (DiCUP/styrene = 1 molar proportion) in the mixture of silane, peroxide, and catalyst reduces the  $\beta$ -scission reaction of the polypropylene. It is known that the amount of styrene added is an extremely sensitive parameter for control of PP-degradation, grafting, hydrolysis, and condensation reaction. Monomeric styrene acts as a radical stabilizer by providing a long-living intermediate radical. 0.03 phr (1 phr (parts per hundred resin): 1 g of

additive mixed into 100 g of polymer) of IRGANOX 1330 (Ciba–Geigy) serves as antioxidant in each of the formulations [6]. The polymer was then shaped into thin sheets (about 1.4 mm thick) and exposed to water at 80 °C for 72 h. In presence of dibutyltin diluarate (DBTL), which acts as a highly efficient catalyst, water molecules transform silyl ether groups (Si–O–R) to silanones (Si–OH) by means of hydrolysis. Neighboring silane grafted groups undergo condensation reaction to form a three-dimensional crosslinked network structure as a precursor for the CSX process.

SCP serves as the swelling fluid for all samples. The critical point of propane is at 96 °C and 4.2 MPa [7].

## 2.2. Experimental procedure

The gel fraction  $\phi_{\text{gel}}$  and the compression modulus  $E$  were chosen as measured parameters to characterize the network polymer. From the compression modulus further network parameters can be calculated [8,9]. The effective network segment concentration  $\nu_e$  is proportional to  $E$  as

$$\nu_e = \frac{E}{3RT} \quad (1)$$

where  $R$  is the universal gas constant and  $T$  is the experimental temperature in absolute scale. The molecular weight between crosslinks  $M_c$

$$M_c = \frac{\rho}{\nu_e} \quad (2)$$

is inversely proportional to the network segment concentration [8].  $\rho$  is the density of the polymer.

The weight fraction of connected network (gel fraction) as compared to the whole sample was determined using an ASTM method [10]. A preweighed sample of mass  $m_0$  was exposed for 72 h to *p*-xylene at 110 °C, which extracted most of the loose chains (sol fraction  $\phi_{\text{sol}}$ ). The gel fraction remained un-dissolved in the vessel. It was recovered and dried for 24 h under vacuum at 80 °C before it was weighed (mass  $m_{\text{sox}}$ ) to calculate the gel fraction and the sol fraction

$$\phi_{\text{gel}} = m_{\text{sox}}/m_0; \quad \phi_{\text{sol}} = 1 - \phi_{\text{gel}} \quad (3)$$

The traditional Soxhlet extraction method [11] was found to be too harsh for samples of such low crosslink density as used in this study. The constant exposure of the samples to fresh boiling *p*-xylene during Soxhlet extraction causes chemical bonds to break, thus reporting an erroneous value of the gel fraction. For this reason, all experiments were done with the ASTM method.

The compression modulus for Eq. (1) was measured at 175 °C, well above the nominal melting temperature of 142 °C, to make sure that the crosslinked samples are in the rubbery state without crystals. Discs of 6.35 mm diameter and height  $H_0 = 1.4$  mm were placed into a linear rheometer (Rheometrics RDS-LA controlled by a Labview program that has been developed by Roland Horst) and compressed at a constant strain rate of  $0.005 \text{ s}^{-1}$ . Strain rate  $\dot{\epsilon}$  and strain  $\epsilon$  are defined with the sample height  $H(t)$ :

$$\dot{\epsilon} = \frac{d(\ln H(t))}{dt}; \quad \epsilon = \ln \frac{H(t)}{H_0} \quad (4)$$

The resulting compression force was measured as a function of the increasing strain  $\epsilon$ . Stress was calculated by dividing the measured normal force by the sample cross-sectional area. The compression modulus is defined as the initial slope of the stress–strain curve.

Initial swelling experiments in a high-pressure view cell helped to determine the temperature and pressure conditions and soak time appropriate for the CSX process. Small samples were placed in the view cell and exposed to SCP. A CCD camera connected to the computer and controlled with Labview was used to record the observations. Experiments were performed with temperatures and pressures starting from 140 °C and 13.6 MPa, respectively. Appreciable swelling (approximately 8–10 times) was observed at 155 °C and 27.5 MPa, which were then chosen as parameters for the entire set of experiments. It was also observed that under these pressure and temperature conditions equilibrium swelling could be reached within 1.5 h with small loss of sol molecules. Thus, 1.5 h was set as the soak time for all the experiments.

For the actual CSX experiments, samples were placed in a pressure vessel and exposed to SCP. After swelling at 155 °C and 27.5 MPa for 1.5 h, the temperature was reduced

Table 1

Hifax CA10, a PP copolymer, used as the base polymer is grafted with organosilane VTMOs and with DiCUP as the initiator. DBTL is used as a catalyst for the crosslinking reaction. A small amount of styrene is added to the polymer to reduce the scission reaction of polypropylene. The identification name of each polymer is given as the amount of VTMOs hyphenated with the amount of peroxide used in the reactive extrusion

Identification name	Hifax CA10	Organosilane VTMOs (phr)	Silane/per oxide ratio VTMOs/DiCUP	Peroxide DiCUP (phr)	Catalyst DBTL (phr)	Styrene (phr)
3-075	1000	3	40	0.075	0.02	0.029
3-066	1000	3	45	0.066	0.02	0.026
3-050	1000	3	60	0.050	0.02	0.019
2-050	1000	2	40	0.050	0.02	0.019
2-044	1000	2	45	0.044	0.02	0.017
2-033	1000	2	60	0.033	0.02	0.013

to 85 °C and held there for the sample to crystallize. Before venting the fluid, the temperature was elevated to 105 °C, which is safely above the critical temperature of propane. The same  $P$ – $T$  conditions were repeated for all samples.

The resulting pore structure after the completion of the CSX process was viewed under a scanning electron microscope (SEM) (JOEL 35 CF). To expose the pore morphology, the samples were broken into halves. In order to prevent the pores from collapsing during breaking, the samples were soaked in methanol overnight and then frozen in liquid nitrogen. The cracked samples were then placed on a support disc and sputter coated with gold for the SEM.

The SEM micrographs were analyzed using a software developed in Labview. Each pore was selected individually and straight lines were drawn from wall to wall passing through the center. The length of the lines was measured and averaged over the entire micrograph to calculate the average pore size of each sample.

The void fraction in each of the porous samples

$$\phi_{\text{void}} = \frac{v_{\text{por}}}{v_{\text{por}} + v_{\text{CSX}}} \quad (5)$$

was measured indirectly. The pore volume and the volume of the solid portion of the sample  $v_{\text{CSX}}$  were measured separately and the void fraction was calculated. To determine  $v_{\text{por}}$ , each sample was soaked in methanol (MeOH) under vacuum. The surface MeOH was dried off and the sample was put in a preweighed airtight vial. The vial was weighed again and the difference in weight from the empty vial was subtracted from the weight of the dry sample to obtain the weight of MeOH absorbed. Using the density of MeOH at room temperature, the volume of MeOH absorbed was calculated. Its volume is assumed to be equate to the total volume of the pores  $v_{\text{por}}$  in the specimen (under the assumption that all the pores were filled with MeOH).

In order to estimate the volume of the solid portion of the sample  $v_{\text{CSX}}$ , the mass of the samples after CSX  $m_{\text{CSX}}$  was measured.  $v_{\text{CSX}}$  was estimated as

$$v_{\text{CSX}} = \frac{m_{\text{CSX}}}{\rho_{\text{bulk}}} \quad (6)$$

assuming that the density of the solid portion of the porous polymer is about the same as the bulk density of the polymer before CSX. Such assumption is considered reasonable, since crystallinity is not significantly affected by CSX (as will be shown below). The mass and volume of the polymer specimen before CSX were measured. From these, the average density of the bulk polymer  $\rho_{\text{bulk}}$  was determined for use in Eq. (6).

The crystallinity before and after CSX was measured by DSC (TA Q1000 series). About 5 mg of sample was crimped in a pan and put in the DSC. Heating and cooling scans were run between 40 and 180 °C. Wide angle X-ray diffraction (WAXD) (MRSEC facility) on the crosslinked samples both before and after CSX provided information

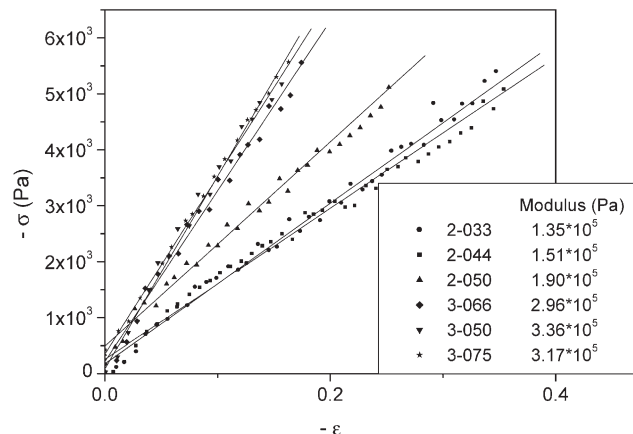


Fig. 1. Compression stress of the silane-grafted crosslinked *i*-PP at 175 °C. The strain is defined as the natural log of the ratio of the deformed height to the initial height.

about their crystal habit. A Cu  $k_{\alpha}$  X-ray beam was used together with a detector that scanned over an angular range of 2° through 40°.

### 3. Results

The gel fraction  $\phi_{\text{gel}}$  of the six samples varies between 29.9 and 48.5 wt%, sample 2-033 having the lowest and 3-075 having the highest (Table 2). The amount of crosslinking increases in the set of samples depending on the amount of VTMOs and DiCUP used [12].

Compression experiments were performed on the bulk polymers at 175 °C. The initial slope of the stress strain curve defines the compression modulus of the bulk polymer (Fig. 1). Sample 2-033 exhibits the lowest modulus of  $1.35 \times 10^5$  Pa and the modulus increases with increase in gel fraction (Fig. 2).

The DSC melting temperature of all the samples is about 142 °C. It was observed that the degree of crosslinking does not significantly affect the melting point or crystallinity of the samples (Fig. 3). This result was somewhat unexpected but fits into the overall results as will be discussed below.

The polymer obtained from CSX showed open-cell porous structures in the SEM micrographs (Fig. 4). A large portion of the inside of the sample was scanned to view the distribution of pore sizes. The average pore size calculated from the SEM micrographs (Table 2), varied between 8.28 and 1.25  $\mu\text{m}$ . Also the pore size decreased with increase in gel fraction (Fig. 5).

Although the pore sizes vary greatly for these samples, the void fractions were found to remain almost constant. All CSX samples have a high pore volume fraction between 80 and 86% (Table 2). This implies that the surface area increases with increasing gel fraction due to the decreasing pore size.

WAXD of the crosslinked polymer (figure not shown) has the four reflections (110, 040, 130, and 041 (041

Table 2

The gel content from extraction, compression modulus in linear rheometer and crystallinity in DSC are measured and molecular weight between crosslinks is calculated from the compression modulus data according to Eq. (2) for the crosslinked polymer before swelling. After the CSX process, Percentage weight remaining and void fraction are measured. The approximate pore sizes are obtained from the SEM pictures over a large scan of area. Sample code as in Table 1

Sample	Crosslinked polymer				Polymer after CSX		
	Gel content (%)	Compression modulus ( $\times 10^5$ Pa)	Crystallinity (%)	$M_c$	Percentage weight remaining after CSX	Void fraction	Approx. pore size ( $\mu\text{m}$ )
2-033	29.9	1.35	10.85	72297	68.18	0.86	7.24
2-044	33.6	1.51	9.42	64639	66.89	0.85	8.28
2-050	37.0	1.90	11.46	51371	77.01	0.83	8.11
3-066	44.9	2.96	11.40	32975	84.81	0.84	3.51
3-050	46.7	3.36	11.20	29049	81.08	0.85	2.74
3-075	48.5	3.17	8.62	30790	68.82	0.80	1.25

overlapping with 131)) that are typical for  $\alpha$ -PP. Only  $\alpha$ -PP crystals were formed in the samples. It was also interesting to find that the WAXD peaks of the porous polymer after CSX are identical with the four WAXD peaks of the bulk polymer. The supercritical fluid in the CSX process does not affect the crystal structure as probed with DSC and WAXD. WAXD reflections of  $\beta$ -PP crystals were not noticeable.

The same set of experiments was performed on the pure network polymer from which the sol fraction had been extracted according to the ASTM method. The goal was to find more information on the role of the network in the pore formation. The DSC heating scans on these pure network samples show no distinct  $i$ -PP peaks at all, i.e. the gel fraction of the polymer was found to be completely amorphous. This agrees with the observation that, in the absence of loose chains, the sample collapses during CSX without formation of any porous structure.

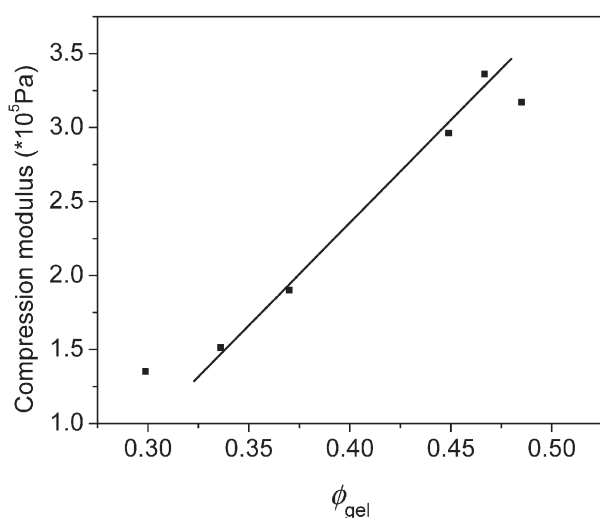


Fig. 2. Compression modulus increases with increase in gel fraction. Thus, the molecular weight between crosslinks  $M_c$  decreases with increase in gel fraction.

## 4. Discussion

### 4.1. Effect of crosslinking

The network polymer by itself was found to be amorphous. This can be attributed to the following. Silane groups preferably graft onto PE segments in the copolymer and less onto the  $i$ -PP segments, where they would cause chain scission at high probability. As a consequence, molecules of high PE copolymer content are more likely to participate in the grafting reaction but, later in the CSX, these molecules cannot readily crystallize because of their highly irregular composition along the molecular backbone. These more highly grafted molecules have a higher probability to connect into the network structure. The selective crosslinking process produces a network that preferably consists of molecular strands of high copolymer fraction and very low crystallinity. The network is non-crystalline since its building blocks (molecular strands) are already non-crystalline. Also, grafted VTMO molecules can be viewed as side chains that additionally hinder the

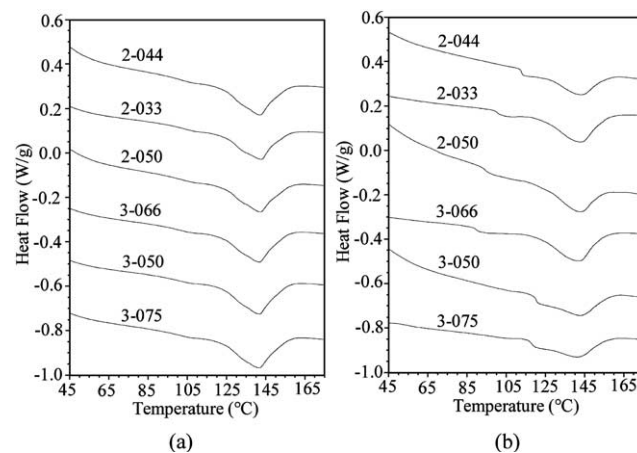


Fig. 3. Heat of fusion (a) before CSX (b) after CSX for different gel fractions. The melting point and the degree of crystallinity do not change with the amount of crosslinking.

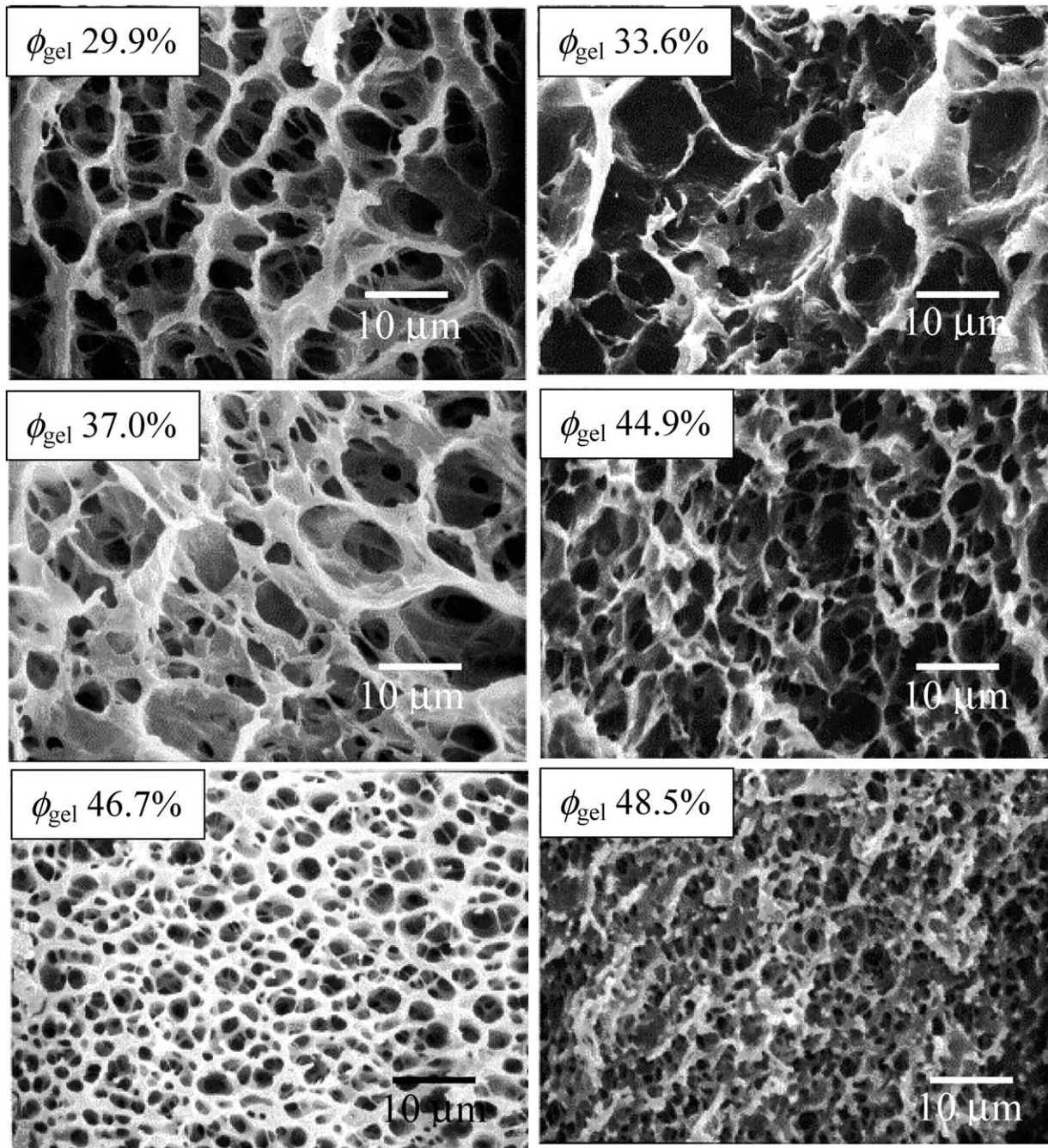


Fig. 4. The six samples show open-pore structures after CSX. For the CSX process, the samples were exposed to SCP at 155 °C and 27.5 MPa for 1.5 h for swelling. Temperature was then reduced to 85 °C for the samples to crystallize. Before venting the fluid, the temperature was elevated to 105 °C, which is safely above the critical temperature of propane. The values indicated in the left top corner of the micrographs are the corresponding gel contents.

molecular packing of the main chains. Molecular segments with side chains are excluded from the crystalline phase.

Molecular mobility also has a selective effect. At 80 °C, far from the glass-transition temperature of *i*-PP, molecular mobility is higher in the amorphous phase than in the crystalline phase. The migration of the water molecules for the hydrolysis reaction to form crosslinks occurs mostly in the mobile amorphous phase, which contains the grafts [12]. The crystalline regions remain unaltered. This results in the network that is predominantly amorphous.

The crystallization was found to occur with the sol molecules. This is attributed to the same selection process as described earlier in the discussion. Molecules of low copolymer content will have fewer grafts per molecule and, hence, will less likely bond into the network. They form the sol fraction. Because of their low defect density, these molecules can readily crystallize.

The combined sol and the gel fractions form an interpenetrating network (IPN) of loose chains (sol molecules) that crystallize within an amorphous polymer

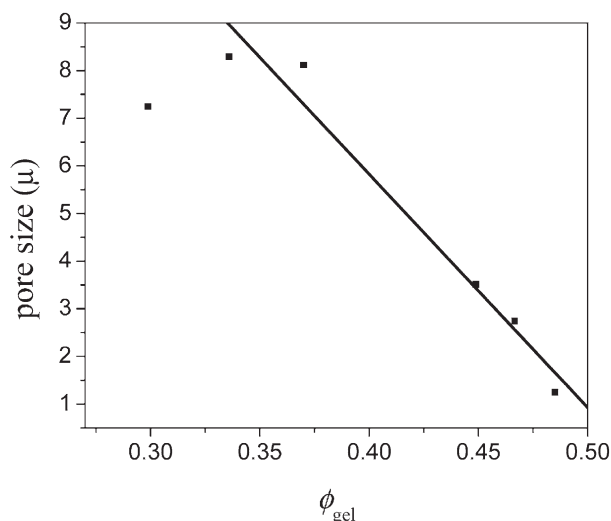


Fig. 5. Variation of pore size with gel fraction. The pore size decreases with increase in gel fraction in the sample. The SEM micrographs of Fig. 4 were analyzed using a software developed in Labview. Each pore was identified individually and straight lines were drawn across them. The length of the lines on every micrograph was measured to calculate the average pore size of each sample. It was observed that the pore sizes decrease with increasing gel fraction. The pore sizes vary from 8.28 to 1.25  $\mu\text{m}$ .

network. The network provides the environment for the crystallization of the unattached polymer molecules. We are not aware of any study of this phenomenon or of reports of such IPNs in the solid state.

#### 4.2. Effect of swelling and mass loss

The rigidity of the pore structure will depend on the amount of crystallizing sol left in the sample after completion of the 'soaking' process. The sol molecules need to be prevented from diffusing out of the sample as much as possible. Soak time and swelling  $P$ – $T$  conditions determine the loss of sol fraction during CSX. The longer the polymer is allowed to sit in the swollen state, the more loose chains migrate towards the sample surface until concentrations in the sample and in the surrounding fluid reach an equilibrium value. The diffusion rate of the loose chains out of the bulk depends on two opposing factors: the distance they have to travel within the bulk before reaching the surface and the diffusivity of the loose chains within the bulk. The characteristic diffusion time increases with the square of the sample thickness, if all other parameters are set constant. Hence, the sol fraction lost within a given time will be much less for a thicker sample (highly swollen) than that for a thinner sample (less swollen). However, the mobility of the sol molecules increases substantially by the presence of the fluid. A highly swollen polymer, as found with low degrees of crosslinking, provides large mesh size in the gel and mobile environment (due to the supercritical fluid). This accelerates diffusion. The two effects are counter active. Because of this, there is an optimum soaking time after which the sample is sufficiently swollen but the sol

molecules have not yet left the sample by large amounts, which need to be aimed for. For this reason, an intermediate soak time of 1.5 h was chosen as optimum for the CSX process. A longer soak time would mean a greater loss of sol molecules.

The two opposing phenomena can be observed quite well in Fig. 6. At low gel fraction (29.9%), the polymer swells enough to provide a substantial diffusion rate which weakens the effect of the larger distance the sol molecules have to travel to reach the surface. Thus the swollen gel loses a large amount of loose chains. As the gel fraction increases, the swelling reduces and lowers the rate of diffusion. Thus, the loss of sol molecules reduces with the increase in gel fraction. In comparison, a much higher gel fraction (46.7 and 48.5%) reduces the swelling and keeps the rate of diffusion small. However, the loose chains have to travel a much smaller distance to reach the surface. The effect of smaller distance overtakes the effect of smaller diffusion rate resulting in an increase in loss of sol molecules.

A large amount of sol molecules (as determined by the ASTM method) was found to be retained in the samples after CSX (Fig. 6). This can be explained by the solvent quality of SCP as compared to  $p$ -xylene that acts as a much better solvent for  $i$ -PP. The amount of swelling of  $i$ -PP in SCP (8–10 times) is much smaller as compared to in  $p$ -xylene (30–35 times). Consequently, the rate of diffusion of the loose chains within the swollen polymer is much smaller in SCP than in  $p$ -xylene. This results in the large retention of sol molecules in the sample within the given soak time in SCP.

Even at very long soak time in SCP, a small fraction of sol molecules was always retained within the network polymer. This may be attributed to the accumulation of sol

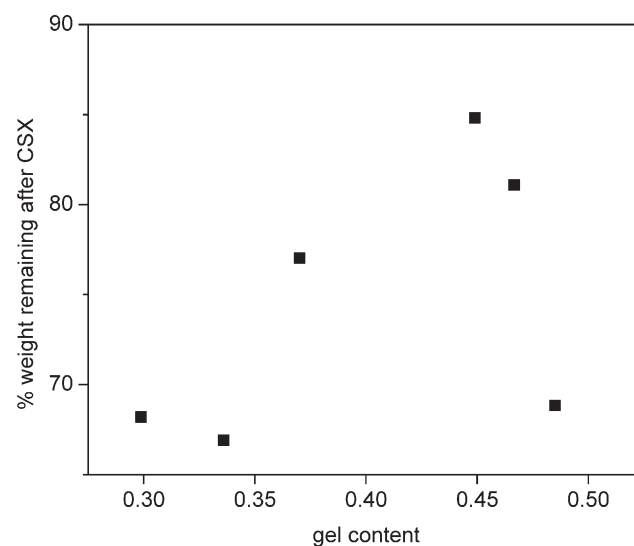


Fig. 6. Percentage weight of polymer remaining after CSX. The ASTM method extracts most of the loose chains leaving behind only the pure network. A large amount of loose chains still remain after CSX, much more than after the extensive extraction.

molecules in the SCP that surrounds the sample inside the pressure vessel. Equilibrium is reached when the chemical potential of the sol in the surrounding bulk fluid equates the chemical potential of the sol within the swollen network.

#### 4.3. Crystallization and pore formation

Polypropylene crystallizes from the melt in a nucleation and growth process [13]. Melt crystallization of partially crosslinked network polyolefins was observed by heating silane-grafted crosslinked polypropylene to 180 °C to reach the rubbery state and then crystallizing it at 120 °C. Spherulitic growth with a high nucleation density was observed under the microscope (Fig. 7). During CSX, a similar nucleation and growth type of behavior of the network polymer is expected. At the onset of crystallization, it is assumed that the sol molecules form the nuclei, resulting into a spherulitic growth. After the crystallization of the sol molecules, the fluid occupies large interconnected regions in the solidified polymer. Non-crystallizing fractions of the sol and the gel may remain in the fluid. The fluid can be removed by simply lowering the pressure. A liquid–liquid phase separation of the three-component system of un-crystallizable sol molecules, the network and the supercritical fluid occurs only during venting, when the pressure is low enough to induce phase separation.

The fluid in the open pores can leave the sample freely during this expansion. Expansion of the fluid is preferably induced above the critical temperature so that surface tension is negligible and the pores do not collapse. Small remnants of the fluid in the amorphous phase may act as a foaming agent. This potentially leads to a foaming process where the fluid trapped in the polymer forms bubbles during

depressurization. Trapping and bubble formation is expected to occur preferably at a rapid drop of pressure and at significantly high temperature. Possible traces of fluid remaining in the porous polymer may get removed by applying vacuum for appropriate times.

The presence of the crystals prevents the pore walls from collapse during the venting of the fluid. This is learned from the CSX experiments on the pure network, which is completely amorphous, and does not form pores during the CSX process. It is assumed that the amorphous system collapses during cooling because of the absence of any rigid structure. The crystals provide rigidity to the structure. The pore walls that are about 50–200 nm thick (Fig. 4) can easily accommodate lamellae of *i*-PP crystals (thickness 15–20 nm) [14] even if they form as twisted ribbons as reported for spherulite growth. But the crystal morphology of the wall could not be confirmed under transmission electron microscopy because the porous samples were too soft for microtoming.

The DSC scans for samples after CSX show shoulders at low temperatures (Fig. 3(b)) that are not present in the melting peaks of samples before CSX (Fig. 3(a)). The low temperature shoulders are assumed to belong to low-melting crystals that have been formed during CSX where the mobility of the chains is higher due to the presence of SCP. This allows some less regular chains (chains containing a few PE copolymer blocks in the backbone) to partially crystallize over the readily crystallizable *i*-PP chains, producing some imperfect crystals. These imperfect crystals melt at a low temperature and appear as a shoulder in the DSC scans. During melt crystallization (no fluid added), such less regular blocks do not crystallize because of lack of molecular mobility. Thus, no shoulders are seen in the melt

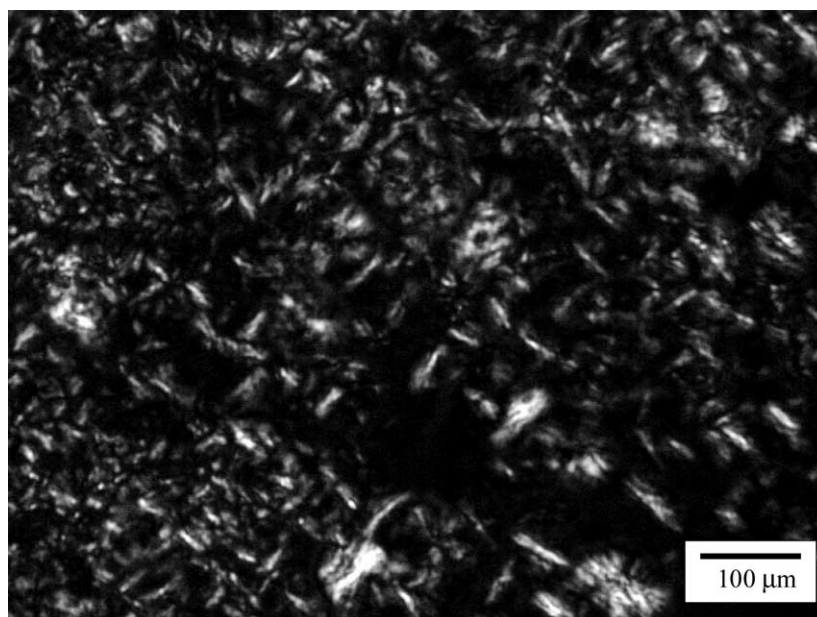


Fig. 7. Spherulites obtained during melt crystallization of partially crosslinked *i*-PP. The sample was heated to 180 °C and then allowed to crystallize at 120 °C. This temperature was chosen so that the crystallization process can be observed under the microscope and recorded using a CCD camera.

peaks of these bulk-crystallized samples. The hypothesis is supported by the second heating scan of specimens after CSX, since the DSC scans do not show the low temperature shoulder. The characteristics became similar to melt crystallized samples.

The polymer density after CSX can be approximated as the bulk density of the polymer,  $\rho_{\text{bulk}} = 0.894 \text{ g/cm}^3$ . This approximation is justified since the polymer crystallinity, of different specimens, as obtained from DSC, does not vary by much (Table 2).

#### 4.4. Influence on pore size

$M_c$ , calculated from  $E$  using Eqs. (1) and (2) (Table 2), provides an average value for the molecular weight between crosslinks. It is expected that polymer molecules containing higher concentrations of copolymer will have molecular strands between crosslinks that are shorter than the calculated value. Similarly the fraction containing lower concentration of copolymer will have longer molecular strands between crosslinks compared to the calculated value. The value of  $M_c$  indicated in Table 2 is only a relative measure of the varying degree of crosslinking between the samples. It is observed that  $M_c$  decreases with increase in gel fraction, implying an increasing number of shorter chains in the network. This contributes toward the increase in compression modulus with increase in gel fraction.

SEM micrographs show that pore sizes decrease with increase in gel fraction. Thus a qualitative relationship between the molecular weight between crosslinks and the average pore size is obtained. The pore sizes decrease with decrease in molecular weights between crosslinks.

## 5. Conclusion

The results of this study show that the open pore structures obtained during the CSX process have high void fraction (80–86%) with pore sizes of the order of 1–10  $\mu\text{m}$ . The pore sizes decrease with increase in gel fraction of the sample, as seen from the SEM micrographs. The use of gel fraction as a measure of crosslink density is supported by rheological measurements. The compression modulus increases with gel fraction, which is explained by a decrease of molecular weight of strands between crosslinks. This suggests that the pore sizes increase with the increase in molecular weight between crosslinks.

Silane groups preferably graft onto *i*-PP/PE copolymer in segments with high PE copolymer content, since peroxides cause  $\beta$ -scission in *i*-PP segments along with radical

formation. Molecules with high PE copolymer content remain in the amorphous phase because of their highly irregular composition. Thus, the resulting network formed from the crosslinking of the grafts is non-crystalline. The sol molecules consisting of low PE copolymer content readily crystallize during CSX and provide rigidity to the pore structure.

CSX is a novel process for obtaining open-pore structures in *i*-PP. The sample can be preshaped, crosslinked and put through CSX to obtain porous specimens of desired shape and size. The amount of gel fraction of the sample decides the pore size of the final product. The pressure and temperature effects on the CSX process are currently under study.

## Acknowledgements

We thank the National Science Foundation (NSF/CTS-0107156) for funding this project and Basell Polyolefins for providing the polypropylene samples. We are also grateful to MRSEC for WAXD facilities and Alan Waddon for helping with wide angle X-ray diffraction experiments.

## References

- [1] Winter HH, Gappert G, Ito H. *Macromolecules* 2002;35:3325–7.
- [2] Flory PJ. *Principles of polymer chemistry*. Ithaca: Cornell University Press; 1953. p. 576–580.
- [3] Whaley PD, Kulkarni S, Winter HH, Stein RS, Ehrlich P. *Polymeric materials science and engineering. Proceedings of the ACS Division of Polymeric Materials Science and Engineering* 1995;73:404.
- [4] Whaley PD, Kulkarni S, Ehrlich P, Stein RS, Winter HH, Conner WC, Beaucage G. *J Polym Sci, Part B: Polym Phys* 1998;36(4):617–27.
- [5] Han SJ, Lohse DJ, Radosz M, Sperling LH. *J Appl Polym Sci* 2000; 77:1478–87.
- [6] Fritz HG, Bolz U, Lu R. *Int Polym Process XIII* 1998;2:129–35.
- [7] Tester JW, Modell M. *Thermodynamics and its applications*, 3rd ed. New Jersey: Prentice Hall PTR; 1983. Appendix G.
- [8] Dinzbarg BN. *Elastomers Plastics* 1999;52(9):413–9.
- [9] Flory PJ, Rehner J. *J Chem Phys* 1943;11(11):512–20.
- [10] Structural test methods for determination of gel fraction and swell ratio of crosslinked ethylene plastics. ASTM designation D2765-90; 1990.
- [11] Sajkiewicz P, Phillips PJ. *J Polym Sci, Part A: Polym Chem* 1995;33: 853–62.
- [12] Anderlik R. *Herstellung thermoplastischer elastomere auf der basis silanvernetzter polypropylen/ethylene-propylene-elastomer-mischungen*. Institut für Kunststofftechnologie. PhD Thesis, University of Stuttgart, Germany; 1994, p. 34–37.
- [13] Padden FJ, Keith HD. *J Appl Phys* 1959;30:1479.
- [14] Sano H, Usami T, Nakagawa H. *Polymer* 1986;10:1497–504.